small NANO MICRO

Nanowires

Site-Specific Self-Assembled Liquid-Gated ZnO Nanowire Transistors for Sensing Applications

*Vivek Pachauri, Alexis Vlandas, Klaus Kern, and Kannan Balasubramanian**

***A** scalable bottom-up solution-based approach for the site-specific realization of ZnO nanowire (ZnO-NW)-based field-effect transistors for sensing applications in liquids is reported. The nanowires are grown across predefined electrodes patterned by photolithography. Site specificity is attained by the use of nanoparticles acting as seeds. Using integrated on-chip microchannels and microfabricated gate electrodes, electrochemically gated ZnO-NW network transistors functioning in liquids are demonstrated. The optimized devices are rendered sensitive to pH through chemical functionalization. The unique combination of the sensitivity, site specificity, scalability, and cost effectiveness of the technique opens up avenues for the routine realization of one-dimensional nanostructure-based chemical and biosensors for analytical and diagnostic applications.*

Keywords:
- chemical sensors
- field-effect transistors
- liquid gating
- site-specific growth
- ZnO nanowires

1. Introduction

Semiconductor nanowires (s-NWs) are ideal building blocks for a variety of applications, including nanoscale chemical and biosensors.[1] In this context, s-NWs can be deployed as electrical detectors, showing promise for single-molecule detection, high sensitivity, and large-scale integration.[2] A wide range of sensors based on s-NWs have been realized, almost all of which rely on a transduction mechanism based on the electric-field effect.[3] Carbon nanotubes (CNTs) are promising alternative candidates for the realization of nanoscale sensors in liquids.[4] Although synthesis methods that exclusively provide semiconducting tubes are only beginning to emerge for CNTs,[5] s-NWs do not face this problem. Among the various s-NWs, ZnO nanowires (ZnO-NWs) have attracted special interest due to the possibility of simple low-temperature growth in solution and the ensuing applications.[6,7] For sensing with s-NWs, the back-gated configuration is widely employed.[3] However, when working in liquids, the use of a gate electrode that is in contact with the liquid provides clear benefits, as has been demonstrated for CNT-based sensors.[4,8] In a liquid environment, the size of the electrochemical double layer becomes comparable to the diameter of a one-dimensional (1D) nanostructure. This gives a good capacitive coupling, which leads to a very effective gating of the transistor channel.[9] In addition to reducing the operating voltages, the electrochemical gating method provides a precise way to control the electronic filling level of the nanosystem, thus minimizing hysteresis effects. Until now, the potential of the electrochemical gating method remains largely unexplored for ZnO-NW-based field-effect transistors (FETs).[2]

While FETs fabricated using ZnO-NWs have been thoroughly investigated, and their use as miniaturized sensors demonstrated in a number of prototypes, the successful realization of sensors for marketable applications still remains a far-off dream. One of the major barriers to achieving this goal is the difficulty in positioning the nanowires or fabricating sensors at any desired location.[10,11] While these hurdles have been overcome for Si nanowires via the fabrication of sensor arrays,[2] ZnO-NW-based sensors operating in liquids are only beginning to emerge.[12] The ZnO-NWs are usually produced ex situ from various synthesis methods,[7,13–18] requiring the use of a different substrate. As a result, the wires need to be transferred from the growth substrate into a dispersion via scratching or sonication, which are not easy to scale up.

[*] Dr. K. Balasubramanian, V. Pachauri, Dr. A. Vlandas, Prof. K. Kern
Max Planck Institute for Solid State Research
Heisenbergstraße 1, 70569 Stuttgart (Germany)
E-mail: b.kannan@fkf.mpg.de
Prof. K. Kern
Institut de Physique des Nanostructures
Ecole Polytechnique Fédérale de Lausanne
1015 Lausanne (Switzerland)

Supporting Information is available on the WWW under http://www.small-journal.com or from the author.

DOI: 10.1002/smll.200900876

Techniques for the site-specific growth of ZnO-NWs in a large scale are thus vital for the successful realization of application-specific devices. A number of different approaches have been proposed for the large-scale device assembly of ZnO-NWs, which include trapping by AC dielectrophoresis[11] and lateral growth from locations predefined by patterning and lithography.[19,20]

In this Full Paper, we demonstrate an efficient ''bottom-up'' approach for the realization of liquid-gated ZnO-NW-based FETs combining site-specific growth with high performance. These two aspects make this method ideally suited for cost-effective large-scale production. In the first step, we show an optimized, low temperature, solution-based growth procedure for obtaining ZnO-NWs with a small diameter distribution using nanoparticles as growth seeds. Secondly, we demonstrate the site-specific fabrication of low-resistance FETs across photolithographically defined electrodes by employing the optimized growth procedure. Following this, we discuss the liquid-gated electronic transport characteristics of the self-assembled ZnO-NW FETs inside microchannels. Our architecture provides for high performance in liquids with ON/OFF ratios close to 10^4, and a subthreshold swing as low as 105 mV decade^{-1}. Finally, we demonstrate functional pH sensors employing the optimized devices.

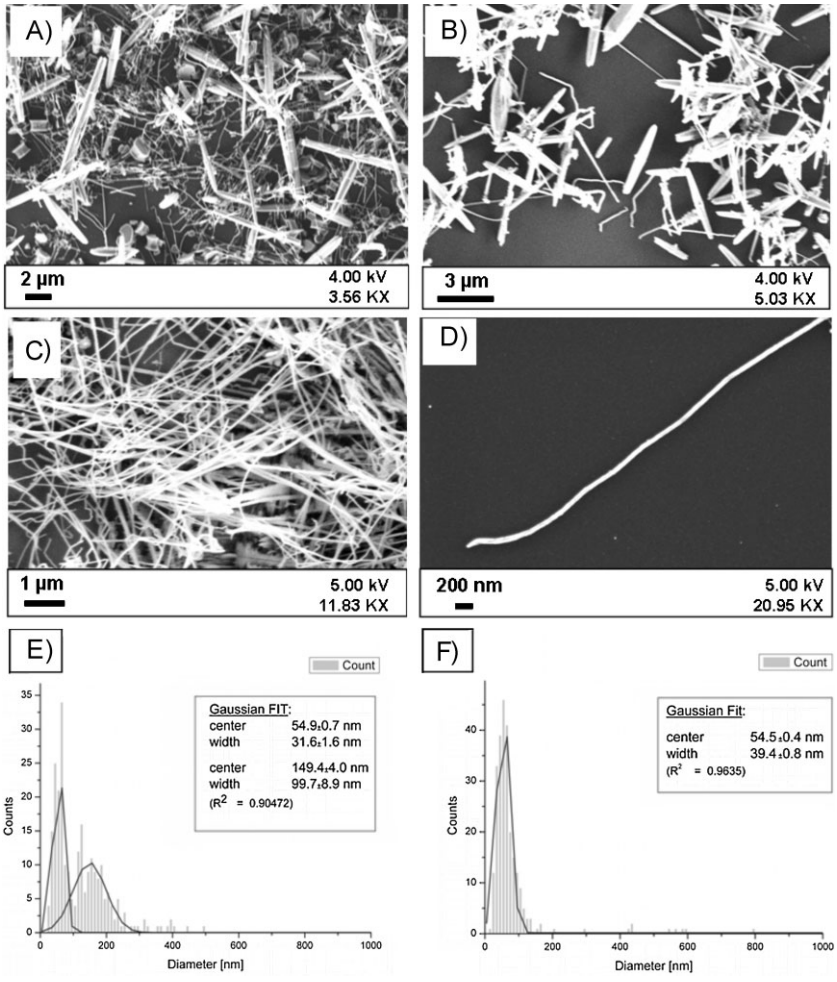

Figure 1. SEM images of ZnO nanostructures grown on seeded (Au colloids) Si/SiO_2 substrates using A,B) the *standard* and C,D) the *modified* solution-based growth procedure. The images show samples after 44 h of growth in an aqueous solution of zinc nitrate and HMTA at 85 °C. E,F) Diameter distribution of ZnO wires grown using E) the standard method and F) the modified growth procedure. The standard method produces wires with a very broad distribution of diameters, a large proportion of which are more than 100 nm. By contrast, the optimized procedure yields nanowires with a tighter unimodal diameter distribution and an average diameter of around 54 nm.

2. Results and Discussion

2.1. Controlled Solution Growth of Homogeneous ZnO-NWs

ZnO-NWs can be grown at very low temperatures in aqueous solutions by hydrolysis of zinc salts.[21] Although chemical bath deposition methods show great potential for employment in large-scale applications, such attempts to grow nanowires often result in a mixture of products of different shapes and sizes. Figure 1A and B shows scanning electron microscopy (SEM) images of ZnO-NWs synthesized using zinc nitrate and hexamethylenetetraamine (HMTA).[22] For this purpose, Si/SiO_2 substrates coated with ZnO or gold nanoparticles were placed in a precursor solution containing 0.25 mM zinc nitrate and 0.25 mM HMTA at 85 °C for 44 h in a convection oven. It is apparent from the images that two types of nanostructures are formed in the growth process: (i) ZnO-NWs of a small diameter (<100 nm), and (ii) spindle-like ZnO microscale structures having large diameters (>150 nm). Several runs with differing precursor concentrations and varying seed diameters did not result in ZnO-NWs with a unimodal diameter distribution. For the applications envisioned here, it is important to obtain homogeneous ZnO-NWs over large areas, while simultaneously preserving the simplicity and effectiveness[21] of the HMTA-based growth procedure.

To understand the growth mechanism, SEM images (see Supporting Information) were obtained at consecutive growth times at a fixed precursor concentration and temperature. These observations lead us to conclude that spontaneous growth leading to spindle-like structures happens within the first four hours after the start of the reaction, and seeded growth follows subsequently. One possible reason could be the limited diffusion of active species towards the nanoparticles that are present on the surface, thereby restricting the growth to a later period of time. On the basis of this growth mechanism, we designed a modified solution growth method whereby Si/SiO_2 substrates coated with the nanoparticles were introduced into the reaction mixture 4–5 h after the start of the reaction. Figure 1C and D shows representative SEM images taken on

NANO MICRO small

such substrates. The images indicate clearly that homogeneous ZnO-NWs with a high aspect ratio (at least 100) can be obtained using this growth technique, while simultaneously minimizing the proportion of spindle-like structures. Further support for the homogeneous distribution of the obtained wires was gathered by detailed analyses of the diameters of the ZnO-NWs from SEM images, as shown in Figure 1E and F. It can be inferred that the standard method provides for both small- and large-diameter wires, while our modified method is efficient in providing a unimodal distribution with an average diameter as low as 54 nm.

2.2. Site-Specific Fabrication of ZnO-NW-Based FETs

Towards the aim of realizing ZnO-NW devices at any desired location, we devised a fabrication procedure, as shown in Figure 2A. Metal electrodes (Pt, 100 nm) are patterned and deposited by standard photolithography on a 4-inch Si wafer with thermally grown SiO_2 (600-nm thickness). After the fabrication of the electrodes, the wafer is cut into smaller substrates ($4 \times 4\,mm^2$) for nanowire growth. The choice of photolithography enables the reuse of the same mask, thus paving way for very low fabrication costs, in contrast to electron-beam lithography (EBL). In a second step, the growth seeds are deposited on the electrodes via alternating-current (AC) dielectrophoresis. The advantage here is that the seeds can be deposited exclusively on the electrodes, and thus the growth is confined to the desired locations only. We ensure that the particles are exclusively deposited on the electrode areas close to the gap, by using a trapping configuration (see Figure 2A), where the dielectrophoretic field is maximized close to the gap region. In a third step, the sample is introduced into a growth solution around 4–5 h after the start of the reaction, which guarantees the growth of homogeneous wires from the deposited seeds. After a specified growth time, the nanowires bridge the gap, resulting in the self-assembly of the device. Atomic force microscopy (AFM) and SEM images at various stages of the fabrication of the ZnO-NW device are shown on the right side of Figure 2. Isolated nanoparticles can be clearly observed in Figure 2B after the dielectrophoretic deposition. Figure 2C shows the growth of nanowires at an initial stage from the deposited nanoparticles, while Figure 2D displays a typical final device.

The field-effect characteristics of the self-assembled ZnO-NW devices were subsequently characterized in a back-gated configuration. The as-grown wires always displayed very high resistances (in the GΩ range, see Supporting Information) and a minimal field effect, indicative of nonoptimal contacts and deep-level impurity states introduced during the growth in the form of oxygen vacancies.[23,24] Both of these problems could be mitigated by subjecting the fabricated devices to rapid thermal annealing (RTA) at 800 °C in air for 30 s, or a prolonged annealing at 300 °C for a few hours. The resistance typically decreases by around three orders of magnitude using this procedure. Further support for the presence of structural defects in the as-grown wires and their removal upon annealing has been gathered by transmission electron microscopy (TEM; see Supporting Information).

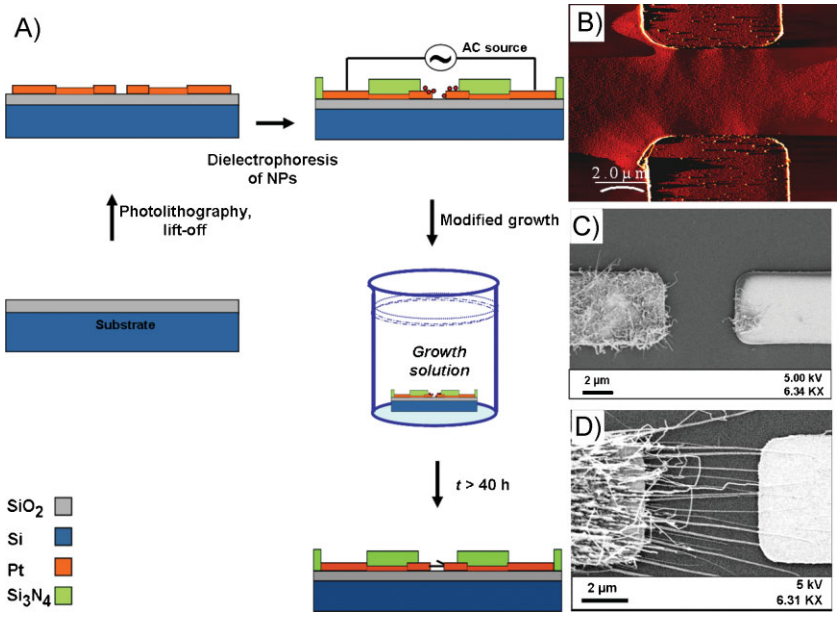

Figure 2. A) Schematic image showing the procedure for the site-specific fabrication of ZnO-NW FETs. Pt electrodes are prepared on Si/SiO_2 wafers by standard photolithography methods. Following this, growth seeds (Au or ZnO nanoparticles) are trapped on selected electrodes by AC dielectrophoresis. The samples are subsequently introduced into the growth solution 4.5 h after the start of the reaction (modified growth). After around 40 h, ZnO-NWs are found to bridge the electrode gaps. B) AFM image showing isolated Au nanoparticles trapped on the Pt electrodes. C) SEM image showing initial stages of the nanowire growth, where it can be clearly seen that they start to grow from the deposited seeds. D) SEM image of a typical final device obtained using this procedure.

2.3. Liquid-Gated Electronic Transport in ZnO-NW FETs

With the aim of the realization of FETs in liquids, microfluidic channels were integrated on the Si/SiO_2 wafers containing the electrodes. In contrast to standard methods, where the channel is usually prepared using a separate slide made of polydimethylsiloxane (PDMS),[2] we used a direct method for realizing the channels. For this purpose, a 10-μm-thick silicon nitride layer was deposited by plasma-enhanced chemical vapor deposition on wafers prefabricated with Pt electrodes. Channels (30 μm wide), reservoirs, and access holes for the pads were carved out of the silicon nitride layer using reactive ion-beam etching with the help of a second etching mask. A schematic of the resulting sample, with optical and confocal microscopy images of the channel with the electrodes, is shown in Figure 3A–C. The final cut sample ($4 \times 4\,mm^2$) contained four structures, each of them consisting of three sets of electrodes and one microchannel connected to two reservoirs. The channel contained source and drain electrodes with a 5-μm gap where the nanowires could be grown, and a gate electrode for measuring

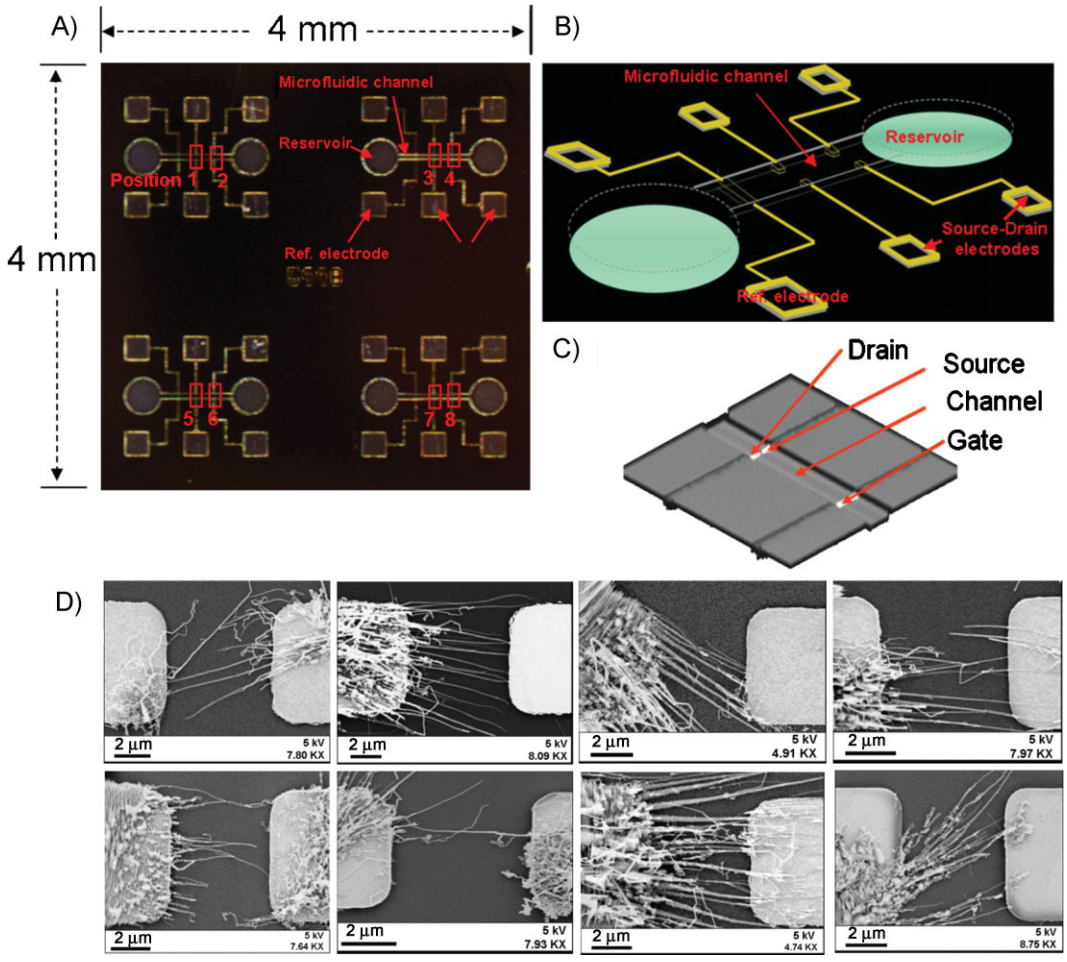

Figure 3. A) An optical image showing a $4 \times 4\text{-mm}^2$ sample comprised of 4 structures. The square pads, the horizontal microchannel, and the circular reservoirs are clearly visible. B) Schematic image showing the integrated microchannel made of silicon nitride on top of the electrodes fabricated as in Figure 2. The microchannel, reservoirs, and access holes for the contact pads are obtained by reactive ion etching through a patterned mask. C) A confocal 3D projected optical image of the integrated microchannel with the source/drain electrodes (incorporating the gap) and the liquid-gate electrode. D) SEM images showing the growth of the nanowires at 8 different gap positions on the same sample. The images correspond to the positions numbered 1–8 in (A).

the field-effect characteristics in liquids. The ZnO-NWs were grown as described earlier, followed by an annealing step at 800 °C in air for 30 s. Figure 3D shows SEM images of 8 different gap positions on the same substrate after growth, where it is apparent that all of the gaps are bridged by a few nanowires. This corresponds to a density of 8 devices per $4 \times 4\ \text{mm}^2$ of the sample, representing a good basis for the realization of on-chip sensor systems for lab-on-a-chip applications.

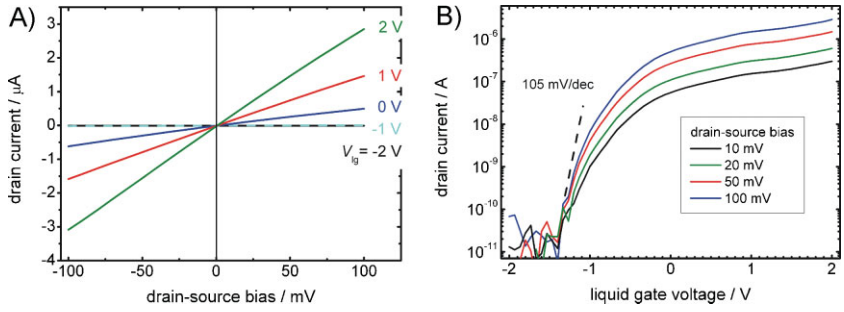

Figure 4. Electrochemically gated electronic transport characteristics of the site-specifically fabricated ZnO-NW network FETs in deionized water: A) *I*–*V* characteristics of a ZnO-NW network device at different liquid-gate voltages. B) Liquid-gate dependence of the drain current at various drain–source biases.

The liquid gating experiments were conducted by spotting a drop of deionized water in the reservoir, which led to the filling of the channel. Figure 4 shows typical liquid-gated field-effect characteristics of the fabricated transistors. The FETs show n-type transport characteristics with a conductance that can be modulated by 4–6 orders of magnitude. The subthreshold slopes of the devices were in the range of 105–200 mV decade^{-1}. The best values for subthreshold slope reported until now are of the order of 130 mV decade^{-1}.[25,26] However, most of these devices are comprised of individual nanowires randomly contacted by tedious EBL, or utilize complex device architectures, which

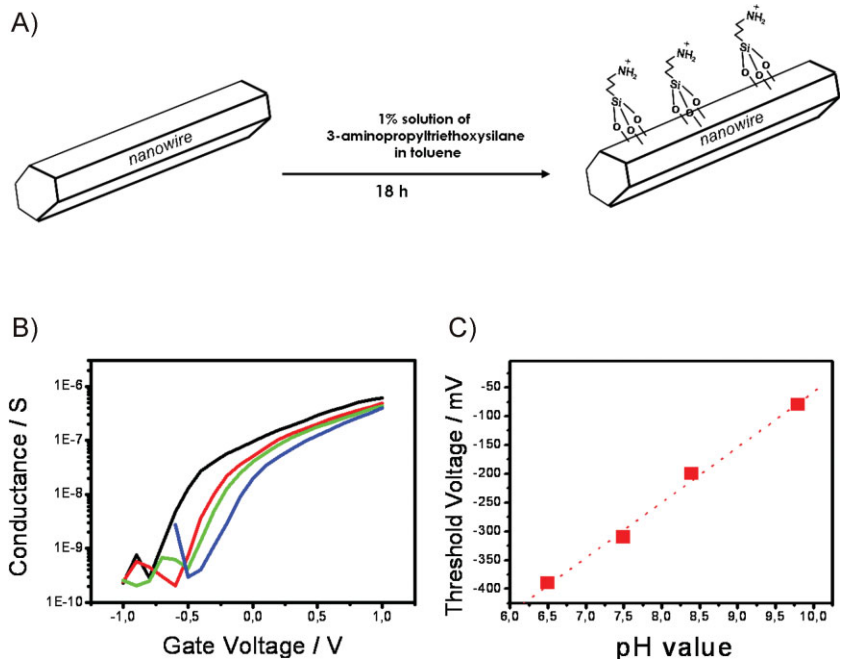

Figure 5. pH sensors using site-specific ZnO-NW FETs: A) Schematic of the chemical functionalization of the ZnO-NWs with 3-aminopropyltriethoxysilane to obtain pH-sensitive functional groups on the surface. B) Gate dependence of the conductance of the functionalized device in various pH buffer solutions. C) Calibration plot showing the threshold voltage of the device as a function of solution pH.

cannot be scaled up easily, and hence are not appropriate for marketable applications. The switching behavior in most of our devices is like that of a depletion-mode transistor, with the device in the ON state at zero gate voltage, which is a common characteristic in almost all of the reported ZnO-NW-based transistors. The gate leakage through the liquid medium was far below 100 pA in a gate voltage range of ±2 V. The transconductance of the device in Figure 4 was found to be more than 1 μS at a drain bias of −100 mV. For a network of 20 wires with a diameter of around 50 nm, we obtain a normalized transconductance of 0.02 S cm^{-1}, which is comparable to high-performance nanorod transistors reported with a transconductance around 0.015 S cm^{-1}.[25,27]

The field-effect mobility (μ) of electrochemically gated FETs can be calculated in a similar fashion to that of their back-gated counterparts. It is given by $\mu = (dI_d/dV_{lg})\ L/(V_{ds}\ c_{edl})$, where I_d is the drain current, V_{lg} is the liquid gate voltage, L is the channel length (5 μm in our samples), V_{ds} is the drain bias, and c_{edl} is the capacitance per unit length due to the electrical double layer, as given by $c_{edl} = 2\pi\varepsilon_r\ \varepsilon_0/\ln(1+\lambda_D/r)$.[28] ε_r is the dielectric constant of the liquid (80 for water), λ_D is the Debye length, which is a function of ionic strength (around 4–5 nm for deionized water[29]), and r is the radius of the ZnO-NW. In this manner, the field-effect mobility of the device in Figure 4 has been calculated to be 1.85 cm^2 (Vs)$^{-1}$. While higher values have been reported with back-gated individual wires that were either covered or functionalized,[25,27] or used a nanoscale air gap,[26] this is the first report of a mobility value for a self-assembled ZnO-NW network transistor operating based on the electrochemical field effect in liquid.

2.4. pH Sensors Based on ZnO-NW FETs

Now, we turn to the demonstration of a pH sensor based on the fabricated ZnO-NW FETs. For this purpose, the self-assembled ZnO-NWs were functionalized in a 1% toluene solution of 3-aminopropyltriethoxysilane for 18 h. This rendered the surface of the nanowires with pH-sensitive groups. Figure 5 shows the sensor response to different buffer solutions with varying pH. It is apparent that the threshold voltage of the device continuously shifts as a function of pH. The results are consistent with an ion-selective FET mechanism,[30] whereby the charge of the amino groups on the surface of the functionalized nanowires introduces a voltage offset that is reflected as a pH-dependent threshold-voltage shift.

3. Conclusion

In summary, we have demonstrated a "bottom-up" approach for the site-specific fabrication of high-performance ZnO-NW-based FETs operating as sensors in liquids. Homogeneity, and, thereby, reproducibility in the preparation of the nanostructures, was achieved by using a delayed growth technique employing an aqueous chemical bath at low temperatures. The ZnO-NW devices were self-assembled by placing growth seeds at predefined locations through inexpensive photolithography. The device characteristics of the fabricated devices could be optimized by RTA. The obtained FETs show low resistances (in the MΩ range), and display excellent device characteristics. They were rendered sensitive to pH through chemical functionalization. These results show that the proposed method constitutes a versatile and cost-effective approach for the large-scale realization of ZnO-NW-based chemical and biosensors in liquids.

4. Experimental Section

Seeds for ZnO-NW growth: A suspension of homogeneous ZnO nanoparticles was prepared based on an existing method.[31] In brief, 1 mM zinc acetate ($Zn(CH_3COO)_2$) was dissolved in 80 mL of 2-propanol under vigorous stirring at 50 °C, followed by dilution to a total volume of 920 mL and cooling in an ice bath. To this solution, 80 mL of 20 mM sodium hydroxide (NaOH) solution in 2-propanol was added under continuous stirring, and the mixture was immersed in a preheated water bath at 50 °C for 2 h. This transparent solution was stored at room temperature and is stable for several months in ambient conditions. The gold seeds were either gold nanoparticles synthesized by a standard Turkevich reduction method[32] or commercially procured gold colloids (Sigma, 7-nm diameter). The average diameter of the ZnO and

Au nanoparticles (from the Turkevich method) were roughly 27 and 21 nm, respectively, as observed from AFM and photoluminescence measurements. For the initial growth experiments, Si/SiO_2 substrates were coated with the seeds by spotting a drop of the seed solution onto the samples and allowing the drop to evaporate. For the fabrication of the devices, the seeds were deposited on prepatterned electrodes by AC dielectrophoresis. An AC field (10 $V_{peak\text{-}to\text{-}peak}$, 10 MHz) was applied across the microelectrodes through probe needles using an Agilent 33250A Function Generator. The seed solution was then spotted on the substrate, and the deposition time was varied from 1 to 2 min in order to obtain the desired number of nanoparticles on the microelectrodes. The nanoparticles are attracted by a positive dielectrophoretic force, and hence are deposited on the surface of the microelectrodes. For the fabrication of the transistors, the sample was thoroughly washed with water after the deposition to ensure that they were present on the surface of the electrodes only.

ZnO-NW growth: Aqueous solutions of zinc nitrate ($Zn(NO_3)_2 \cdot 6H_2O$) and HMTA ($((CH_2)_6 \cdot N_4)$) were used as precursors for the growth of ZnO-NWs in a 1:1 molar ratio (0.25 mM). The growth temperature was maintained at 85 °C throughout the reaction. The samples were left in the growth solution for up to 44 h. For the modified growth procedure, the samples were introduced into the solution 4.5 h after the start of the reaction. At the end of the reaction, the samples were taken out of the solution and cleaned thoroughly with water.

Characterization by microscopy: The nanowires were characterized by SEM and TEM. SEM images were obtained on a Gemini Ultra 55 operating at 4–5 kV. TEM images were recorded using a Phillips CM200 electron microscope operated at 200 kV. For this purpose, the wires grown on Si/SiO_2 substrates (with or without electrodes) were scratched off the surface using a clean razor blade and a drop of ethanol. The resulting suspension was thereafter dispersed on a holey carbon-coated copper grid. AFM images were obtained using a Digital Instruments Dimension 3000 operating in tapping mode. Confocal images were obtained using a Leica TCS SP2 with a laser excitation of 488 nm.

Device fabrication and characterization: The electrodes and the microchannels were fabricated by conventional photolithography techniques at the Institute for Microtechnology (HSG-IMIT, Villingen-Schwenningen, Germany). The fabricated ZnO-NW devices were characterized using a home-made transport measurement system comprised of a 2-channel voltage source (Keithley 2602 for drain bias and gate voltage), a current-to-voltage converter, and a Keithley 2000 multimeter. A manual wafer probe system (Süss Microtec PM5) with probe heads and probe needles was used to contact the pads leading to the electrodes.

Acknowledgements

This work was funded by the German Federal Ministry of Education and Research (BMBF) with project ID O3 X 5516. The authors thank Dr. Peter A. van Aken and Marion Kelsch of the Stuttgart Center for Electron Microscopy (StEM) for help with the TEM measurements.

[1] W. Lu, C. M. Lieber, *J. Phys. D, Appl. Phys.* **2006**, *39*, R387.
[2] F. Patolsky, G. Zheng, C. M. Lieber, *Nat. Protoc.* **2006**, *1*, 1711.
[3] H. J. Fan, P. Werner, M. Zacharias, *Small* **2006**, *2*, 700.
[4] K. Bradley, J. C. P. Gabriel, M. Briman, A. Star, G. Gruner, *Phys. Rev. Lett.* **2003**, *91*, 218301.
[5] M. C. Hersam, *Nat. Nanotechnol.* **2008**, *3*, 387.
[6] Z. L. Wang, *J. Mater. Chem.* **2005**, *15*, 1021.
[7] Z. L. Wang, *J. Phys. Condens. Mater.* **2004**, *16*, R829.
[8] A. Maroto, K. Balasubramanian, M. Burghard, K. Kern, *ChemPhysChem* **2007**, *8*, 220.
[9] K. Balasubramanian, E. J. H. Lee, R. T. Weitz, M. Burghard, K. Kern, *Phys. Status Solidi A* **2008**, *205*, 633.
[10] H. Kind, H. Yan, B. Messer, M. Law, P. Yang, *Appl. Phys. Lett.* **2004**, *84*, 3358.
[11] O. Harneck, C. Pascholski, H. Weller, A. Yasuda, J. M. Wessels, *Nano Lett.* **2003**, *3*, 1097.
[12] B. S. Kang, F. Ren, Y. W. Heo, L. C. Tien, D. P. Norton, S. J. Pearton, *Appl. Phys. Lett.* **2005**, *86*, 112105.
[13] R. S. Wagner, in*Whisker Technology* (Ed.: A. P. Levitt), Wiley, New York **1970**, pp. 15.
[14] J. C. Hulteen, C. R. Martin, *J. Mater. Chem.* **1997**, *7*, 1075.
[15] S. T. Lee, N. Wang, C. S. Lee, *Mater. Sci. Eng. A* **2000**, *286*, 16.
[16] C. H. Liang, G. W. Meng, G. Z. Wang, Y. W. Wang, L. D. Zhang, S. Y. Zhang, *Appl. Phys. Lett.* **2001**, *78*, 3202.
[17] M. H. Wong, A. Berenov, X. Qi, M. J. Kappers, Z. H. Barber, B. Illy, Z. Lockman, M. P. Ryan, J. L. MacManus-Driscoll, *Nanotechnology* **2003**, *14*, 968.
[18] J. Wang, L. Gao, *Solid State Commun.* **2004**, *132*, 269.
[19] J. B. K. Law, J. T. L. Thong, *Nanotechnology* **2007**, *18*, 055601.
[20] S. H. Ko, I. Park, H. Pan, N. Misra, M. S. Rogers, C. P. Grigoropoulos, A. P. Pisano, *Appl. Phys. Lett.* **2008**, *92*, 154102.
[21] L. E. Greene, B. D. Yuhas, M. Law, D. Zitoun, P. Yang, *Inorg. Chem.* **2006**, *45*, 7535.
[22] M. A. Verges, A. Mifsud, C. J. Serna, *J. Chem. Soc. Faraday Trans.* **1990**, *86*, 959.
[23] K. Vanheusden, W. L. Warren, C. H. Seager, D. R. Tallant, J. A. Voigt, B. E. Gnade, *J. Appl. Phys.* **1996**, *79*, 7983.
[24] A. Van Dijken, E. A. Meulenkamp, D. Vanmaekelbergh, A. Meijerink, *Luminescence* **2000**, *90*, 23.
[25] S. Ju, K. Lee, M. H. Yoon, A. Facchetti, T. J. Marks, D. B. Janes, *Nanotechnology* **2007**, *18*, 155201.
[26] S. N. Cha, J. E. Jang, Y. Choi, G. A. J. Amaratunga, G. W. Ho, M. E. Welland, D. G. Hasko, D. J. Kang, J. M. Kim, *Appl. Phys. Lett.* **2006**, *89*, 263102.
[27] W. Park, J. S. Kim, G. C. Yi, M. H. Bae, H. J. Lee, *Appl. Phys. Lett.* **2004**, *85*, 5052.
[28] S. Rosenblatt, Y. Yaish, J. Park, J. Gore, V. Sazonova, P. L. McEuen, *Nano Lett.* **2002**, *2*, 869.
[29] J. H. Back, M. Shim, *J. Phys. Chem. B* **2006**, *110*, 23736.
[30] P. Bergveld, *Sens. Actuators B* **2003**, *88*, 1.
[31] D. W. Bahnemann, C. Kormann, R. Hofmann, *J. Phys. Chem.* **1987**, *91*, 3789.
[32] J. Turkevich, P. C. Stevenson, J. Hiller, *Discuss. Faraday Soc.* **1951**, *11*, 55.

Received: May 24, 2009
Published online: October 19, 2009

